Sensitivity and uncertainty analysis of microstructure–property relationships for compacted powder metals

E. Acar*[1], Y. Hammi[2], P. G. Allison[2], T. W. Stone[2] and M. F. Horstemeyer[2]

In an earlier study, the authors presented a characterisation of the FC-0205 Ancorsteel powders containing 0·6 and 1·0% Acrawax to define the evolution of the failure line and cap surface of the modified Drucker/Prager cap model during compaction. Using the results of that study (i.e. FC-0205 material parameters), this paper presents sensitivity and uncertainty analysis of the microstructure–property relationships for powder metallurgy compaction. It is found for all of the responses of interest (the compressibility curve, the interparticle friction, the material cohesion, the cap eccentricity and the elastic modulus) that the most dominant parameter is the initial (or tap) density. It is also observed that the uncertainty in output parameters for the case of 1% wax is much larger than those for the case of 0·6% wax, due to the large uncertainty in the failure stress (in particular, the compressive failure stress).

Keywords: Powder metallurgy, Sensitivity, Uncertainty, Compaction

Introduction

In recent years, powder metallurgy (PM) techniques have been employed to manufacture various complex shaped engineering components, which are ordinarily difficult to cast or shape by other methods. Automotive parts have been and continue to be the leading application of PM parts. Used primarily for powertrain and transmission components, mechanical PM components, bearings, cams and toothed components are widely used in car and truck industry. Powder metallurgy parts are widely used mainly because of the precise tolerance, suitability and economical advantages the method gives when a high number of components are produced. Among the various metal forming technologies, powder metallurgy is the most diverse manufacturing process. The manufacturing route provides a method for near net final shape of components extremely complex geometries and components of high strength, where subsequent finishing operations are either minimised or eliminated. The die compaction of powders is used in manufacturing components for a broad range of applications. However, if inhomogeneous density distribution occurs during the compaction process, the component will be rejected or will perform badly in its intended use. Thus it is of great interest to be able to accurately predict the mechanical behaviour of the powder during compaction processes.

Computational and mathematical based modelling for describing the mechanical behaviour of powder metals during compaction and sintering densification processes are recognised as significant contributions to improving reliability and quality of PM parts. These techniques provide a valuable tool in predicting green and sintered density distributions, stress distributions, tool loadings, shape distortions during ejection and sintering, and cracks during pressing, unloading and ejection.[1–4] As the accurate modelling of the behaviour of powder during compaction is necessary, identifying the dominant parameters of the model and quantifying the contribution of the uncertainty of each parameter to the uncertainty in the mechanical behaviour of the powder during compaction is a must.

In an earlier study,[5] the authors presented a characterisation of the FC-0205 Ancorsteel powders containing 0·6 and 1·0% Acrawax to define the evolution of the failure line and cap surface of the modified Drucker/Prager cap model during compaction. This paper presents sensitivity and uncertainty analysis of the microstructure–property relationships for compaction of the FC-0205 Ancorsteel powders containing 0·6 and 1·0% Acrawax. The paper is organised as follows. The next section presents a brief description of the modified Drucker/Prager cap model used in compaction analysis. The section on 'Sensitivity analysis' provides the details and the results of the sensitivity analysis, where the dominant parameters of the constitutive model are identified. The section on 'Uncertainty analysis' gives the details and results of the uncertainty analysis, where the overall uncertainty in the mechanical behaviour of the powder is quantified. Finally, the paper culminates with the concluding remarks listed in the last section.

[1]Department of Mechanical Engineering, Faculty of Engineering, TOBB University of Economics and Technology, Sogutozu, Ankara 06560, Turkey
[2]Mississippi State University, Center for Advanced Vehicular Systems, Mississippi State, 39762, MS, USA

*Corresponding author, email acar@etu.edu.tr

Published by Maney on behalf of the Institute
Received 28 August 2009; accepted 4 November 2009
DOI 10.1179/003258909X12573447241509

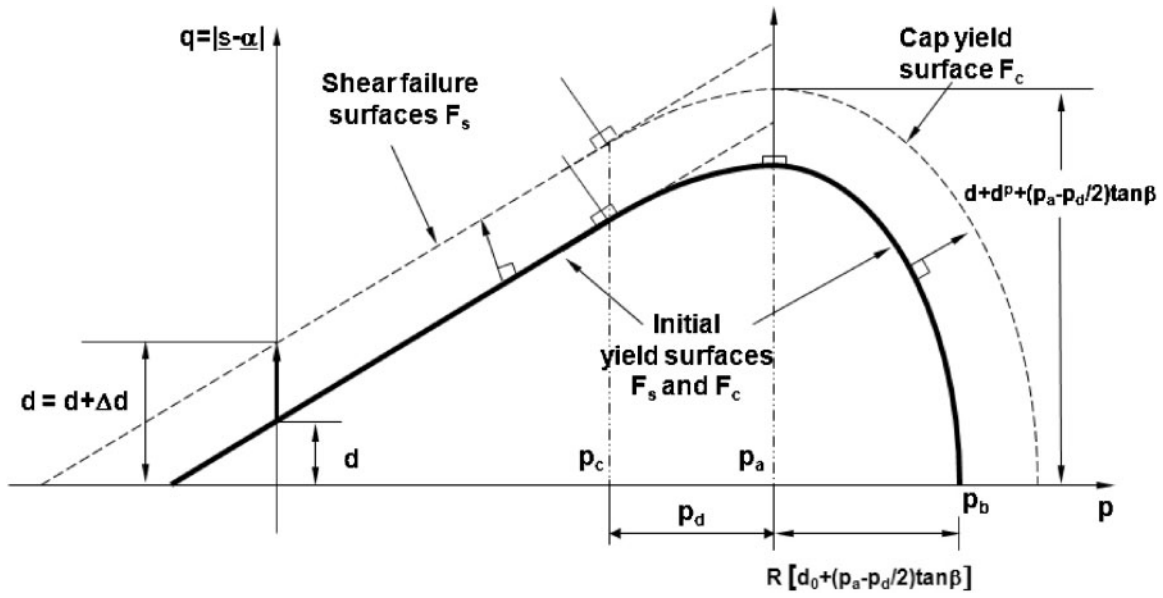

1 Modified Drucker-Prager/Cap model: yield surfaces in $|s\text{-}\alpha|$–p plane

Constitutive model

The modified Drucker-Prager/Cap material model, originally proposed by DiMaggio and Sandler[6] for soil mechanics, is used to define the yield surfaces. The plastic flow is defined by the dissipation potential F_a that is associated with both the cap and the failure yield surface. This double surface plasticity model consists of an elastic region in stress space, bounded by a friction–failure envelope F_a^e in the low pressure region, and an elliptic yield cap F_a^c in the high pressure region. The failure line F_a^e is also influenced by the ductile plastic nature of particles and, therefore, includes the isotropic hardening κ and kinematic hardening α

$$F_a^e = |\underline{s}-\underline{\alpha}| - \kappa - d - p\tan\beta - f_t(p,p_a) = 0 \tag{1}$$

where β is the material's angle of friction and d is its cohesion strength. The failure yield surface is connected to the cap yield surface smoothly using a transition function f_t in the failure yield surface F_s. The pressure dependent transition function f_t is defined by

$$f_t(p) = \frac{H(p-p_c)}{2(p_a-p_c)}[p-p_c]^2\tan\beta \tag{2}$$

where the cap hardening variable p_a is an evolution parameter that represents the volumetric plastic strain driven hardening/softening, and p_c a material parameter that has a small value (Fig. 1).

The cap yield surface F_a^c has an elliptical shape in the meridional ($|s\text{-}\alpha|$, p) plane (Fig. 1) and is written as

$$F_a^c = \left[|s-\alpha|^2 - \frac{1}{R^2}(p-p_a)^2\right]^{1/2} - F_e(d,p_a) = 0 \tag{3}$$

where R is a the cap eccentricity that controls the shape of the cap. The evolution parameter p_a is also defined as a hardening parameter that controls the motion of the cap surface, and p_b defines the geometry of the cap surface. The ellipticity of the cap surface is determined by the material eccentricity parameter R that relates the hardening parameter p_a to p_b through the relation

$$p_b = p_a + RF_e^*(p_a) \tag{4}$$

with

$$F_e^*(p_a) = d_0 + (p_a - \frac{p_c}{2})\tan\beta \tag{5}$$

$$d = \begin{cases} 0 & \text{if } \rho \leqslant \rho_d \\ d_1\exp[d_2(\rho-\rho_d)] - d_1 & \text{if } \rho > \rho_d \end{cases} \tag{6}$$

$$\tan\beta = \begin{cases} b_1 - b_2\rho_d & \text{if } \rho \leqslant \rho_d \\ b_1 - b_2\rho & \text{if } \rho > \rho_d \end{cases} \tag{7}$$

and

$$R = \frac{R_1 - R_2}{1+(\rho/\rho_c)^k} + R_2 \tag{8}$$

where d is the initial material cohesion, and d_1, d_2, ρ_d, R_1, R_2, ρ_c and k are material parameters.[3] Sandler and Rubin[7] proposed a relationship to define the evolution of the cap's motion, which is defined by the isotropic cap hardening rule

$$\bar{\varepsilon}_{vol}^p = W\left\{1 - \exp\left[-c_1(p_b - p_{b|_0})^{c_2}\right]\right\} \tag{9}$$

where p_b the hydrostatic compression yield stress, $\bar{\varepsilon}_{vol}^p$ is the effective volumetric plastic strain, W is the maximum plastic volumetric strain (at hydrostatic compression 'lockup'), c_1 and c_2 are material shape factor parameters, and $p_{b|_0}$ is the initial value of p_b. Using the conservation of mass, the density is derived from the plastic volumetric strain as follows

$$\rho = \rho_0\exp(\bar{\varepsilon}_{vol}^p) \tag{10}$$

where ρ_0 is the initial or tap density.

Sensitivity analysis

Sensitivity analysis is performed to identify the dominant parameters of the constitutive model. Since the analytical formulations for the constitutive model parameters exist (*see* the section on 'Constitutive model'), the sensitivities are evaluated by simply computing the derivatives of the output variables, namely the green density, the interparticle friction, the material cohesion, the cap eccentricity and the elastic modulus.

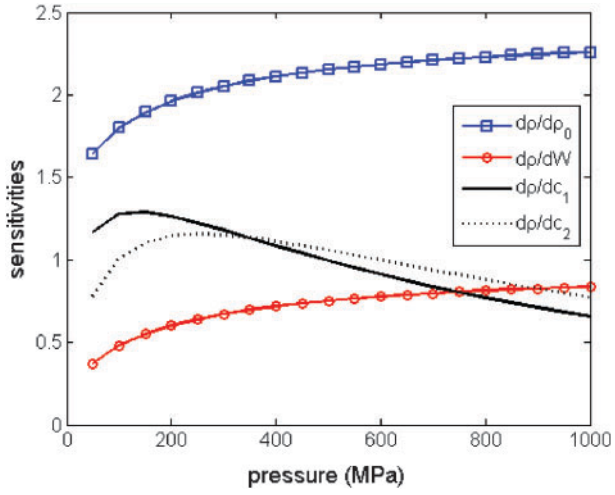

2 Sensitivity of compressibility curve for FC-0205 with 0·6% wax

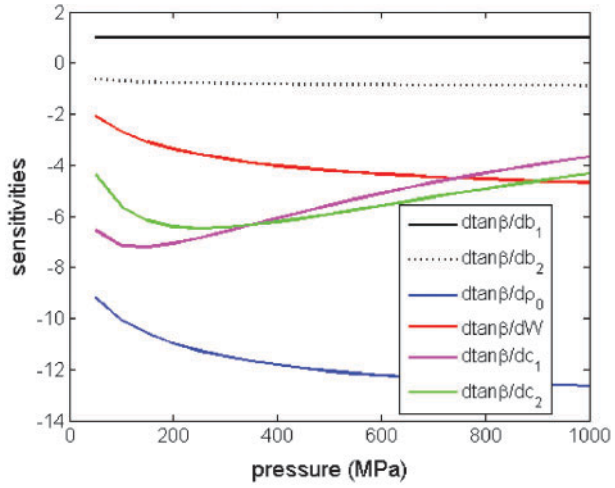

3 Sensitivity of interparticle friction (tan β) for FC-0205 with 0·6% wax

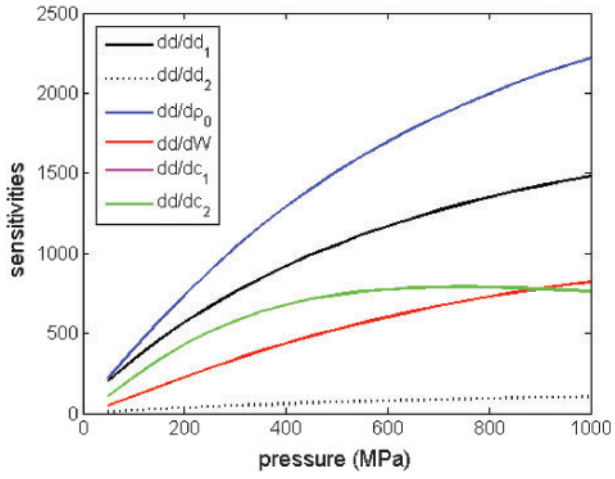

4 Sensitivity of material cohesion (d) for FC-0205 with 0·6% wax

Figures 2–6 show the sensitivity of the compressibility curve, the interparticle friction, the material cohesion, the cap eccentricity and the elastic modulus for FC-0205 with 0·6% wax. For all of the output variables, the most dominant parameter is the initial (or tap) density.

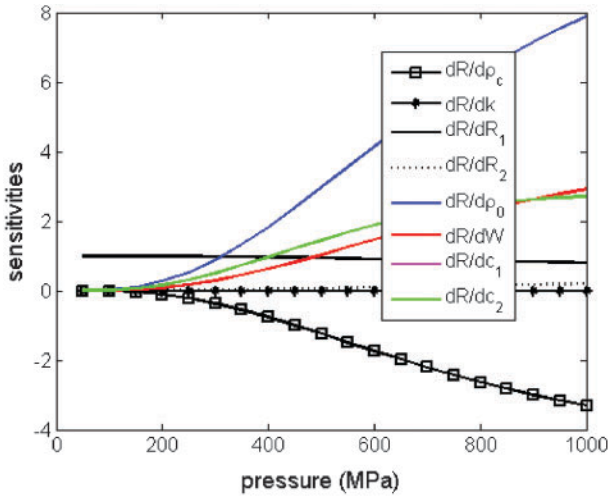

5 Sensitivity of cap eccentricity (R) for FC-0205 with 0·6% wax

Uncertainty analysis

Uncertainty analysis quantifies the overall uncertainty of the output due to uncertainties in the input parameters. To quantify the effect of uncertainties of the model parameters on the material constitutive model, uncertainty propagation based on first order Taylor series expansion (Ang and Tang[8]) is used as given in equation (11)

$$VAR(Y) = \sum_{i=1}^{N} \left(\frac{dY}{dX_i} \right)^2 VAR(X_i) \qquad (11)$$

where VAR stands for variance (a measure of uncertainty, square of standard deviation), X_i is the ith input uncertainty, N is the number of uncertain input variables and Y is the output. Since the analytical formulations exist, uncertainty analysis is computationally inexpensive. If the analytical formulation did not exist and the output parameter calculations were computationally expensive, then the uncertainty analysis would be performed using more efficient techniques (e.g. DR + EGLD technique proposed by Acar *et al.*[9]).

Figure 7 shows that the most of the FC-0205 material test data falls between the 95% confidence bounds.

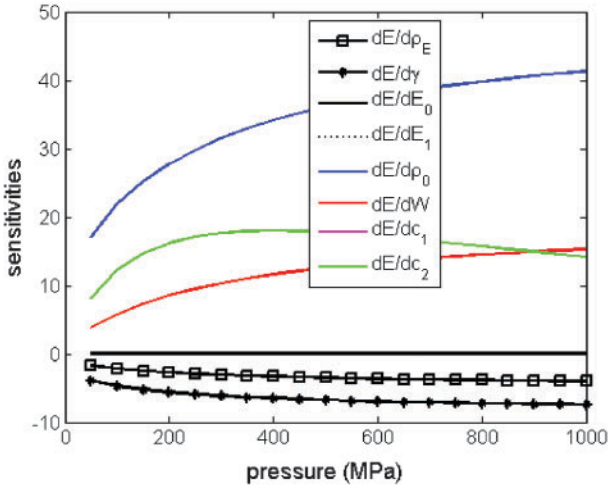

6 Sensitivity of elastic modulus (E) for FC-0205 with 0·6% wax

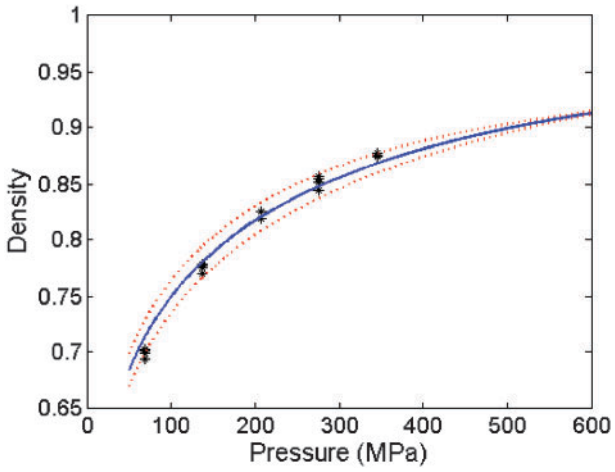

7 Uncertainty in the compression curve for FC-0205 with 0·6% wax

Notice that the uncertainty in the compressibility curve reduces as the pressure is increased.

Figure 8*a* and *b* depicts the variation of uncertainties in the interparticle friction of FC-0205 as the green density changes. The effect of the input uncertainties on the interparticle friction is more profound when 1% wax is used in the powder. Figure 9*a* and *b* illustrates the variation of uncertainties in the material cohesion of FC-0205 as the green density changes. The figures show that increasing the wax in the powder from 0·6 to 1% results in a huge uncertainty in the material cohesion.

The reason for the significant difference between the results of powder with 0·6% wax and the one with 1·0% wax can be explained as follows. The interparticle friction angle is calculated using the failure stress results obtained through compression and tension (Brazilian) tests as given in equation (12)

$$\tan\beta = \frac{q_c - q_t}{p_c - p_t} \tag{12}$$

where p stands for the hydrostatic pressure, q stands for the von Mises equivalent stress, and subscripts t and c refer to tension and compression tests respectively. The hydrostatic pressure and von Mises stress are defined in terms of the failure stresses measured in the tension and compression tests through equations (13) and (14)

$$\text{(for compression tests) } p_c = \frac{\sigma_c}{3},\ q_c = \sigma_c \tag{13}$$

$$\text{(for Brazilian tests) } p_t = \frac{2\sigma_t}{3},\ q_t = (13)^{1/2}\sigma_t \tag{14}$$

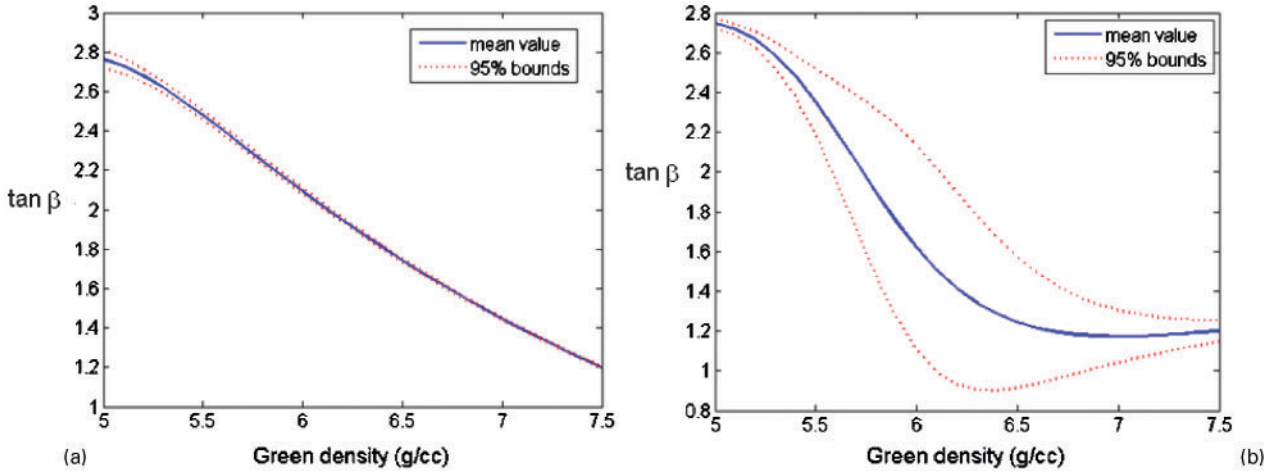

a 0·6% wax; *b* 1·0% wax

8 Uncertainty in interparticle friction for FC-0205 with different wax amounts

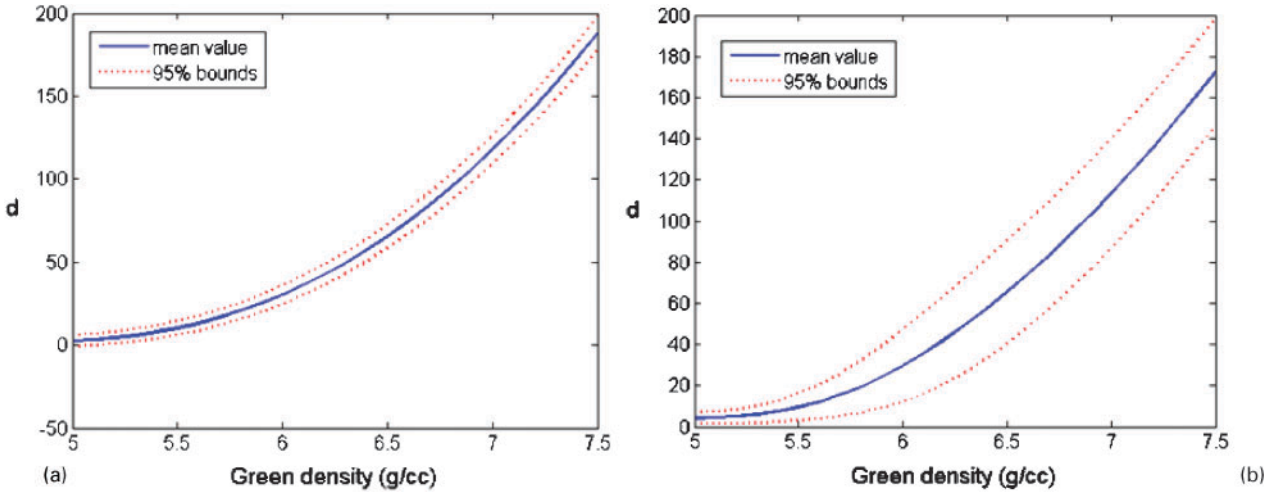

a 0·6% wax; *b* 1·0% wax

9 Uncertainty in material cohesion for FC-0205 with different wax amounts

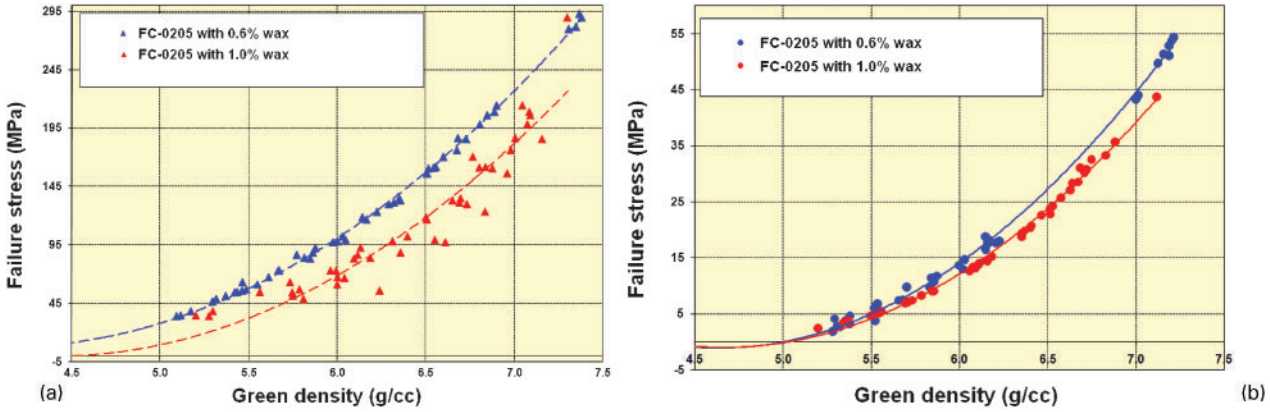

a compression tests; *b* Brazilian tests

10 Failure stress experimental data

Combining equations (11)–(14), the variability in the friction angle can be obtained through

$$VAR(\tan\beta) = \left(\frac{\partial \tan\beta}{\partial \sigma_c}\right)^2 VAR(\sigma_c) + \left(\frac{\partial \tan\beta}{\partial \sigma_t}\right)^2 VAR(\sigma_t) \quad (15)$$

where the uncertainty terms $VAR(\sigma_c)$ and $VAR(\sigma_t)$ are obtained using the test results depicted in Fig. 10. The uncertainty in the results of powder with 1·0% wax (in particular, the compression tests) is much larger than that of the powder with 0·6% wax.

Concluding remarks

This paper presented sensitivity and uncertainty analysis of the microstructure–property relationships of the FC-0205 Ancorsteel powders containing 0·6 and 1·0% Acrawax for compaction analysis. The results obtained from this study led to the following conclusions.

1. Sensitivity analysis indicated that for all of the output variables (the compressibility curve, the interparticle friction, the material cohesion, the cap eccentricity and the elastic modulus), the most dominant parameter is the initial (or tap) density. This showed that for accurate compaction analysis models, an accurate assessment of the initial density is a must.

2. Uncertainty analysis showed that small variations in initial density could lead to large variations in the outputs (the compressibility curve, the interparticle friction, the material cohesion, the cap eccentricity and the elastic modulus).

3. The uncertainty in output parameters for the case of 1% wax was found to be much larger than those for the case of 0·6% wax. The large uncertainty in 1% wax case was mainly due to the large uncertainties in the failure stress obtained from the experiments (in particular, compression tests).

References

1. Y. S. Kwon and K. T. Kim: *Trans. ASME J. Eng. Mater. Tech.*, 1996, **118**, 448–455.
2. R. M. German: 'Sintering theory and practice'; 1996, New York, Wiley and Sons.
3. O. Coube and H. Riedel: *Powder Metall.*, 2000, **43**, (2), 123–131.
4. T. Kraft and H. Riedel: *Powder Metall.*, 2002, **45**, (3), 227–231.
5. Y. Hammi, L. Tucker, P. G. Allison, T. W. Stone, M. F. Horstemeyer and E. B. Marin: Proc. PM World Cong. 2008, Washington, DC, USA, June 2008, Metal Powder Industries Federation, Paper 2008-01-0381.
6. F. L. DiMaggio and I. S. Sandler: *J. Eng. Mech.*, 1971, **97**, (EM3), 935–950.
7. I. S. Sandler and D. Rubin: *Int. J. Numeri. Analy. Meth. Geomech.*, 1979, **3**, 173–186.
8. A. H. S. Ang and W. H. Tang: 'Probability concepts in engineering: emphasis on applications to civil and environmental engineering', 2nd edn; 2006, New York, Wiley.
9. E. Acar, K. Solanki, M. Rais-Rohani and M. F. Horstemeyer: Proc. ASME IDETC/CIE 2008, New York, NY, USA, August 2008, ASME, Paper DETC2008-49168.